Electronic Supplementary Information

Tandem copper and gold nanoclusters for two-color ratiometric explosives detection

Jeremy B. Essner,[‡a] Xi Chen,[‡a] Troy D. Wood,[b] and Gary A. Baker*[a]

[a] Department of Chemistry, University of Missouri, Columbia, MO 65211. E-mail: bakergar@missouri.edu

[b] Department of Chemistry, University at Buffalo, Buffalo, NY 14260

‡ These authors contributed equally to this work.

Experimental Section

Chemicals and Reagents. Hexahydro-1,3,5-trinitro-1,3,5-triazine (RDX, ERR-001S, 1000 μg mL^{-1} in acetonitrile), pentaerythritol tetranitrate (PETN, P-037, 1000 μg mL^{-1} in acetonitrile), 2,4,6-trinitrotoluene (TNT, ERT-022S, 1000 μg mL^{-1} in acetonitrile), 4-nitrotoluene (4-NT, 47242, 1000 μg mL^{-1} in acetonitrile, analytical standard), 2,4-dinitrotoluene (DNT, 101397, 97%), nitrobenzene (NB, 06084, Pestanal®, analytical standard), L-glutathione reduced (GSH, G4251, ≥98.0%), copper(II) nitrate trihydrate ($CuNO_3$, 61194, puriss. p.a., 99-104%), L-ascorbic acid (AA, 05878, TraceSELECT®, ≥99.9998% metals basis), acetonitrile (CH_3CN, 34998, UHPLC Plus, for gradient elution, ≥99.9%), tetrachloroauric(III) acid trihydrate ($HAuCl_4 \cdot 3H_2O$, 520918, ≥99.9% trace metals basis), sodium hydroxide (306576, pellets, semiconductor grade, 99.99% trace metals basis), and bovine serum albumin (BSA, A7030, essentially fatty acid free, essentially globulin free, ≥98% by agarose gel electrophoresis) were all purchased from Sigma-Aldrich (St. Louis, MO) and were used as-received without further purification. Aqueous solutions were prepared from freshly drawn ultrapure water from a Direct-Q 3 UV system polished to a resistivity of 18.2 MΩ·cm.

Synthesis and purification of AuNCs@BSA. The AuNCs@BSA were synthesized following a protocol previously reported by our group.[1, 2] First, 15 mL of 10 mM $HAuCl_4$ (*aq.*) was mixed with 15 mL of freshly prepared 50 mg mL^{-1} BSA (*aq.*). After stirring at 450 rpm for ~ 2 min, 1.5 mL of 1.0 M NaOH (*aq.*) was added under constant magnetic stirring (also at 450 rpm). The reaction mixture was incubated at 38 °C for 24 h to generate the AuNCs@BSA. The as-prepared AuNCs were purified *via* dialysis (Slide-A-Lyzer dialysis cassette, Thermo Scientific, 2 kDa molecular weight cutoff) against 18.2 MΩ·cm water for 48 h. The purified AuNCs@BSA were stored at 4 °C for future use.

Synthesis and purification of CuNCs@GSH. 2.0 mL of 10 mM $Cu(NO_3)_2$ (*aq.*) was added dropwise to 2.0 mL of 50 mg mL^{-1} (162.7 mM) GSH solution (*aq.*) at room temperature under magnetic stirring at 450 rpm. Immediately upon the addition of the Cu^{2+} solution, the solution turned a faint yellow and displayed weak red fluorescence when exciting with a 408-nm laser pointer. The solution was stirred at 450 rpm for an additional 5 min, after which,

0.532 mL of a freshly prepared 120 mM AA solution (*aq*.) was added, followed by a 0.32 mL addition of 1.0 M NaOH (*aq*.), which caused the yellow color to darken (occurred in under 1 min). The solution was then heated at 37 °C under magnetic stirring (450 rpm) for 24 h, after which the solution color had changed from the deep yellow color to brown with a white precipitate sedimenting out (which is tentatively attributed to Cu(I)-GSSG complexes observed in the MS analysis). Next, 1.0 M NaOH (*aq*.) was titrated into the solution (original pH of 2–3) until the pH reached 6.5. Note that during this final addition of NaOH, the white precipitates attributed to the Cu(I)-GSSG complexes re-dispersed. Lastly, the mixture was incubated for another 5 h at 37 °C under 450 rpm magnetic stirring, during which a green solution formed that emitted cyan when exciting with a 408-nm laser pointer. To purify the solution, the as-prepared product was first passed through a 0.2 μm nylon syringe filter (Fisherbrand™ Syringe Filters, Cat. No. 09-719C) to remove any large particulates and any possible insoluble precipitates that remained. The filtrate was then lyophilized for 24 h and the freeze-dried solid was re-dispersed in ~150 μL 18.2 MΩ·cm water. The concentrated solution was then loaded onto an Illustra™ NAP™-25 column (Sephadex™ G-25 DNA Grade) using 18.2 MΩ·cm water as the eluting solvent. The solution separated into two colored bands, the first of which was green in color and strongly emitted cyan, while the second band displayed a pale red color with extremely weak emission. All eluent collected prior to the green band eluting was non-colored and non-emissive and was, therefore, discarded. Since the green band gave the most intense emission, it was attributed to the formed CuNCs@GSH and was, therefore, collected and stored at 4 °C until needed. The weakly emissive red band was not studied within this work, however, the origin and nature of this product are currently under investigation.

Instrumentation. Absorbance and fluorescence data were collected on a Cary Bio 50 UV-Vis spectrophotometer and Varian Cary Eclipse Fluorometer, respectively. For the fluorescence data collection, the PMT was set at 800 V and the excitation and emission slits were set at 5 and 10 nm, respectively. To obtain the structural information of the CuNCs@GSH, the purified products were subjected to electrospray ionization mass spectrometry (ESI-MS) coupled with Fourier transform ion cyclotron resonance (FT-ICR).

Explosives quenching studies. For the quenching studies, 10 μL of the column-purified CuNCs@GSH were diluted with 986 μL of 18.2 MΩ·cm water, followed by an addition of 4 μL of the dialysis-purified AuNCs@BSA. For any single-probe control studies, the 10 or 4 μL additions of CuNCs@GSH or AuNCs@BSA, respectively, were substituted with 18.2 MΩ·cm water to keep the final NC concentrations consistent. The probe solutions, totaling 1 mL, were pipetted into semi-micro quartz cuvettes (1.4 mL) using the 1 cm dimension as the optical pathlength. Next, the various solutions of explosives (TNT, PETN, DNT, RDX, NB, and 4-NT), prepared at concentrations of 1 mg mL^{-1} in acetonitrile, were titrated into separate cuvettes of the dual-probe mixture at 1.0 μL intervals. After each addition, the fluorescence spectrum was collected, exciting at 390 nm and collecting the emission from 395 to 800 nm. All other fluorometer parameters were kept identical to those mentioned in the Instrumentation section. All fluorescence spectra were blank subtracted and dilution corrected. To generate the Stern-Volmer quenching plots, the fluorescence emission was

integrated over 10 nm slices for the single-probe studies and 50 nm slices for the dual-probe studies centered about the NCs' respective emission maxima and the resulting integrated fluorescence intensities in the presence of TNT (F) were ratioed to the integrated fluorescence intensities in the absence of TNT (F_0) or vice versa for the analysis of the quenching constants (K_{SV}). To generate the ratiometric quenching plots, the fluorescence emission was integrated over 50 nm slices centered about the NCs' respective emission maxima and the integrated fluorescence intensity of the AuNCs@BSA (650±25 nm) was ratioed to the integrated fluorescence intensity of the CuNCs@GSH (500±25 nm). The resulting ratios were normalized to the ratio obtained in the absence of quencher such that all ratiometric sensing plots originate at unity.

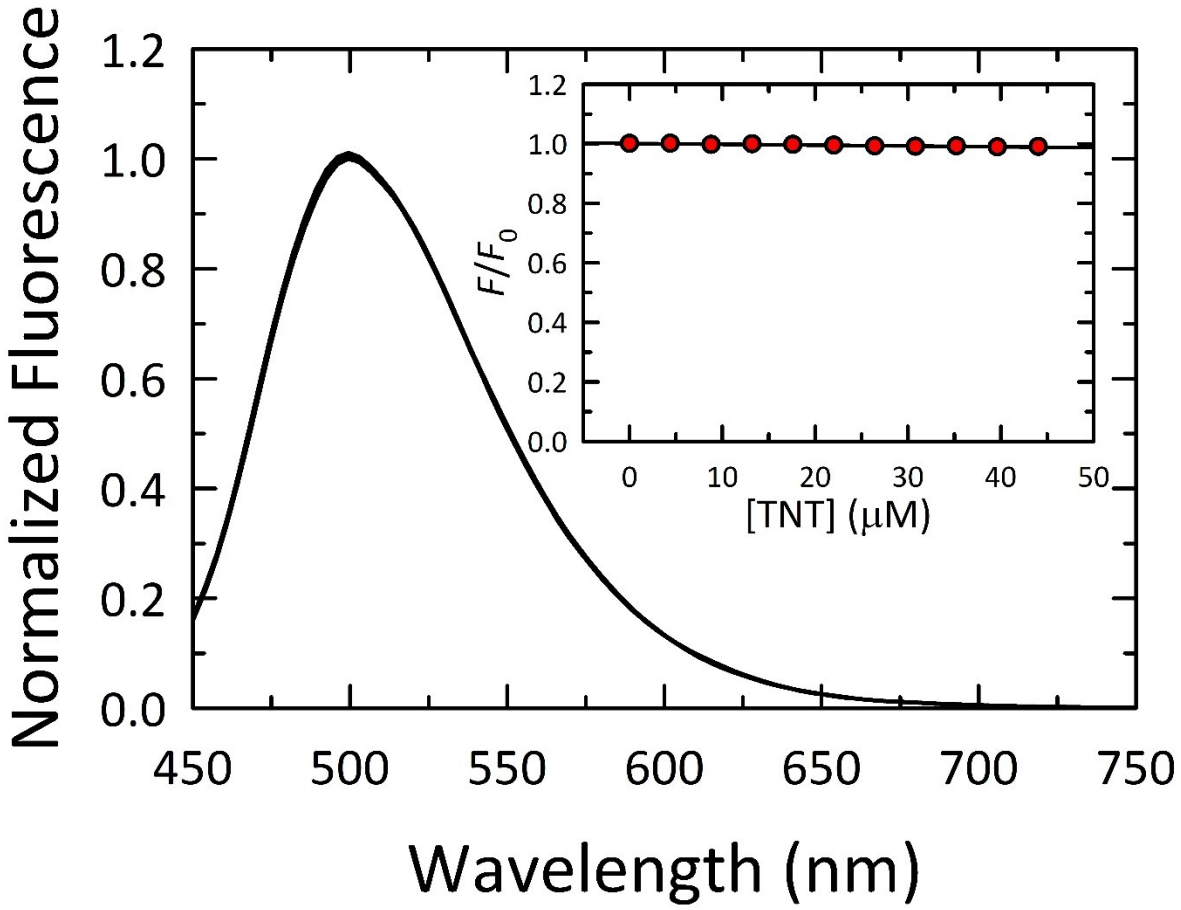

Fig. S1 Normalized fluorescence spectra (excited at 390 nm) of 1 mL of CuNCs@GSH (*aq.*) after each 1 μL addition (ten total additions were made) of 1 mg mL^{-1} TNT in CH_3CN (equating to 0–10 ppm TNT, in 1 ppm increments) highlighting TNT's inability to quench the CuNCs' fluorescence emission. For the inset plot, F/F_0 is the ratio of the integrated CuNC fluorescence emission, where F is the integrated emission in the absence of TNT and F is the integrated emission after each TNT addition. The emission intensity was integrated over 10 nm slices centered about 500 nm.

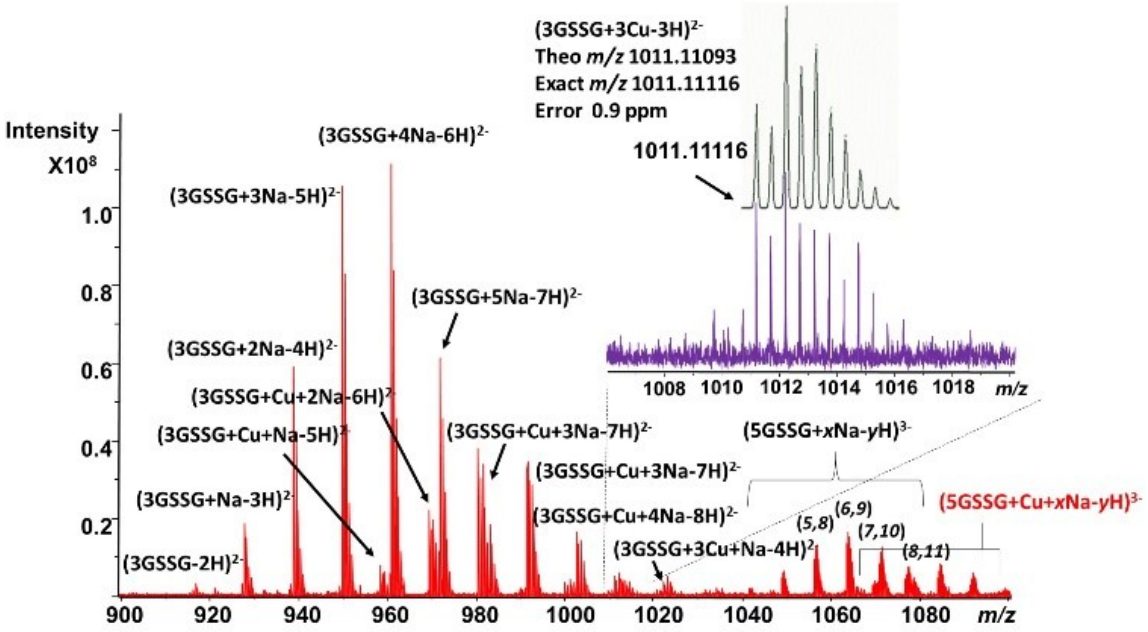

Fig. S2 Negative-ion ESI FT-ICR mass spectrum of the CuNCs@GSH sample in the region *m/z* 900–1100, highlighting the presence of the various sodiated GSSG and sodiated cuprous GSSG complexes as well as demonstrating the successful synthesis of three atom-containing CuNCs.

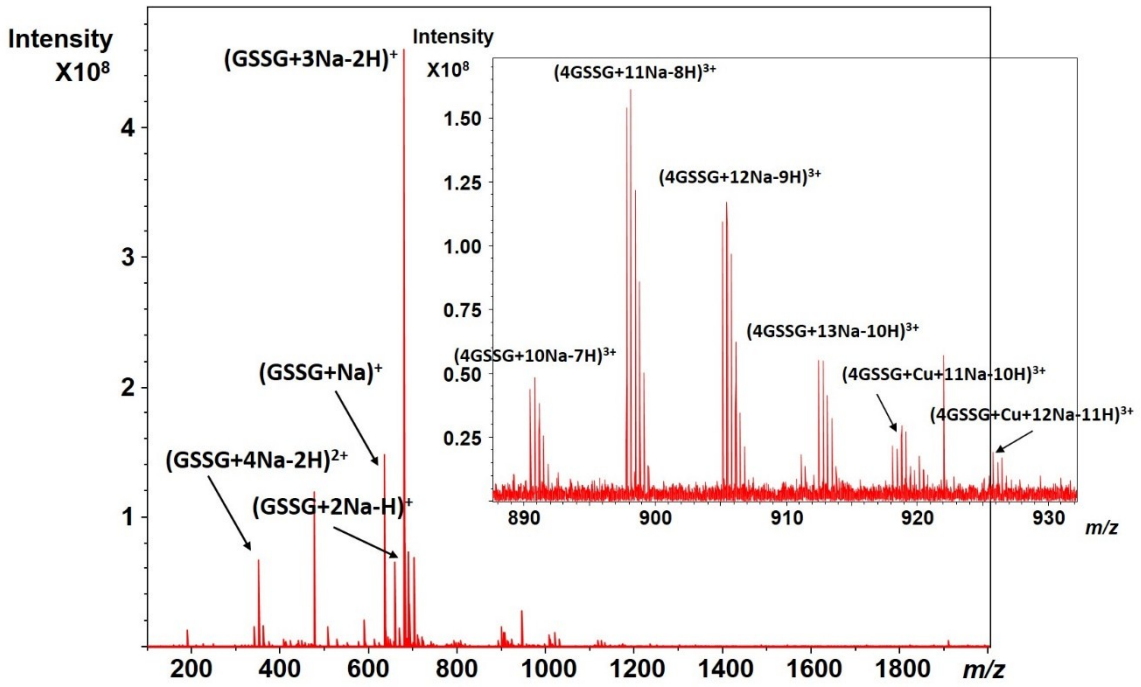

Fig. S3 Positive-ion ESI FT-ICR mass spectrum of the CuNCs@GSH sample in the region *m*/*z* 200–1800 with the inset showing the 890–930 *m*/*z* region.

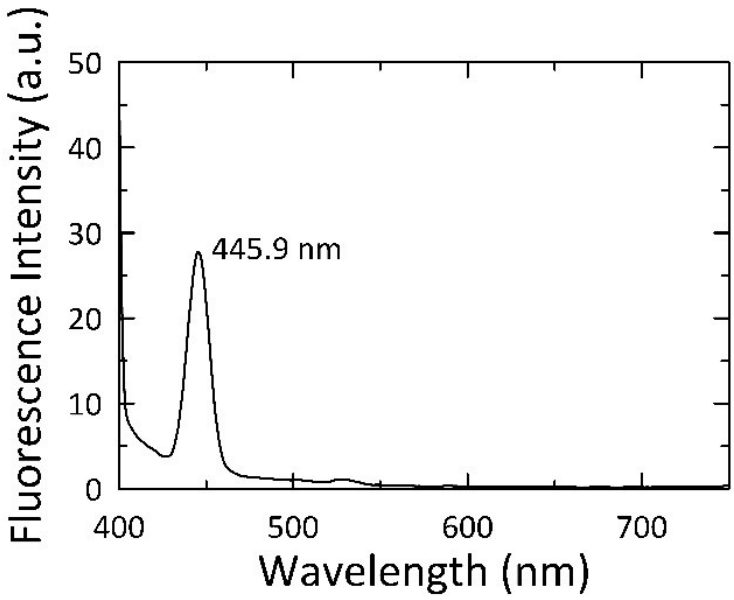

Fig. S4 Fluorescence emission spectra of an 18.2 MΩ·cm solution of water showing the Raman scattering peak of water when exciting at 390 nm, confirming that the slight peak observed on the blue edge of the CuNCs@GSH emission is not due to the NCs but due to solvent scattering (see calculation below).

The Raman scattering band of water will always appear 3390 cm^{-1} red-shifted from the excitation wavelength. Since the dual-probe was excited at 390 nm, the Raman scattering peak of water would appear at:

$$\lambda_{Raman} = \left(\frac{1}{390\ nm} \times \frac{1\ x\ 10^7\ nm}{1\ cm} - 3390\ cm^{-1}\right) \times \frac{1\ x\ 10^7 nm}{1\ cm}$$

$$\lambda_{Raman} = 449.4\ nm$$

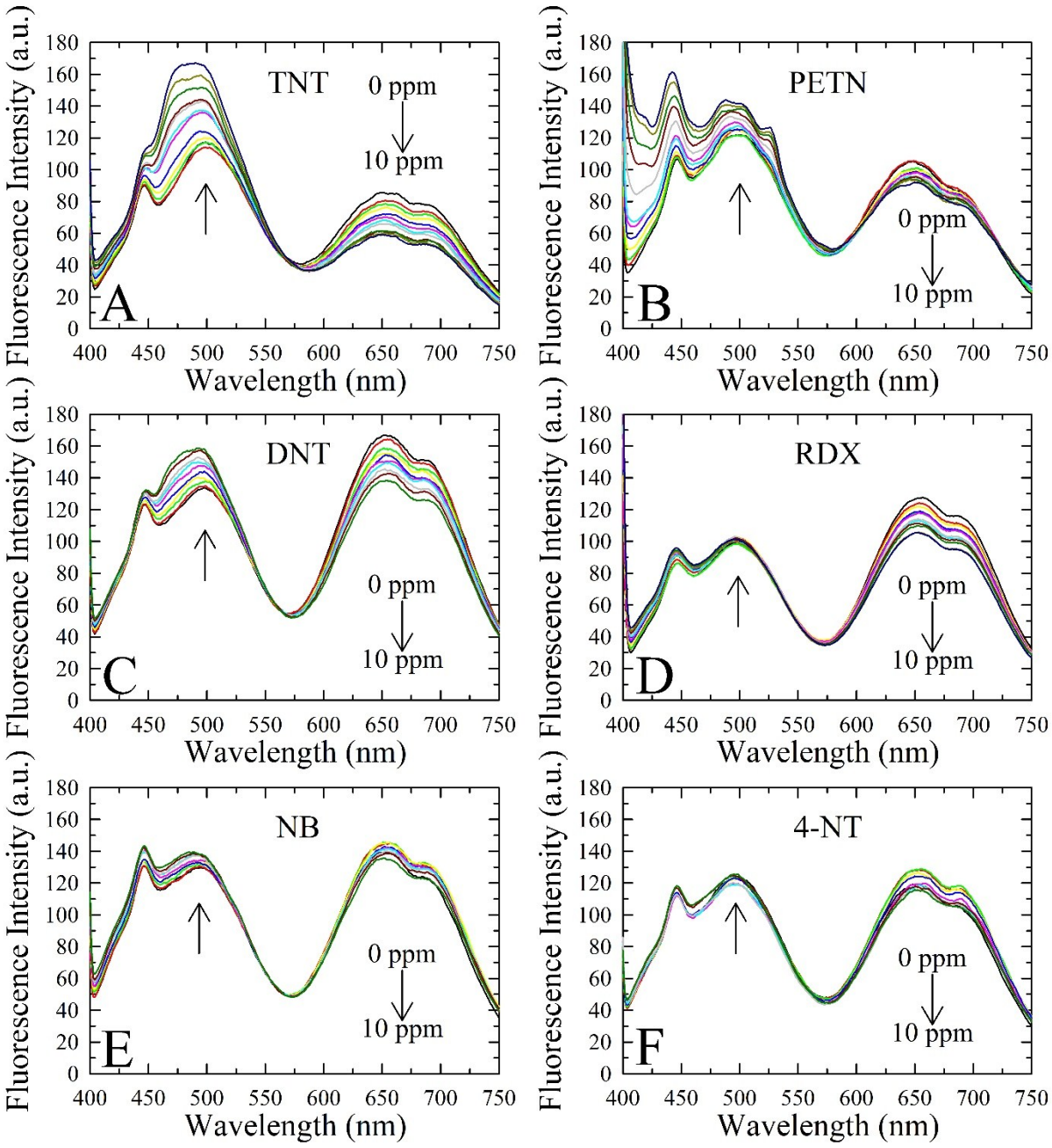

Fig. S5 Representative fluorescence emission spectra (λ_{ex} = 390 nm) of the dual-MNC probe sample in the presence of increasing quantities (0–10 ppm) of (A) TNT, (B) PETN, (C) DNT, (D) RDX, (E) NB, and (F) 4-NT. In general, as the AuNCs@BSA peak was quenched, the CuNCs@GSH emission was systematically enhanced, especially in the presence of TNT, PETN, and DNT.

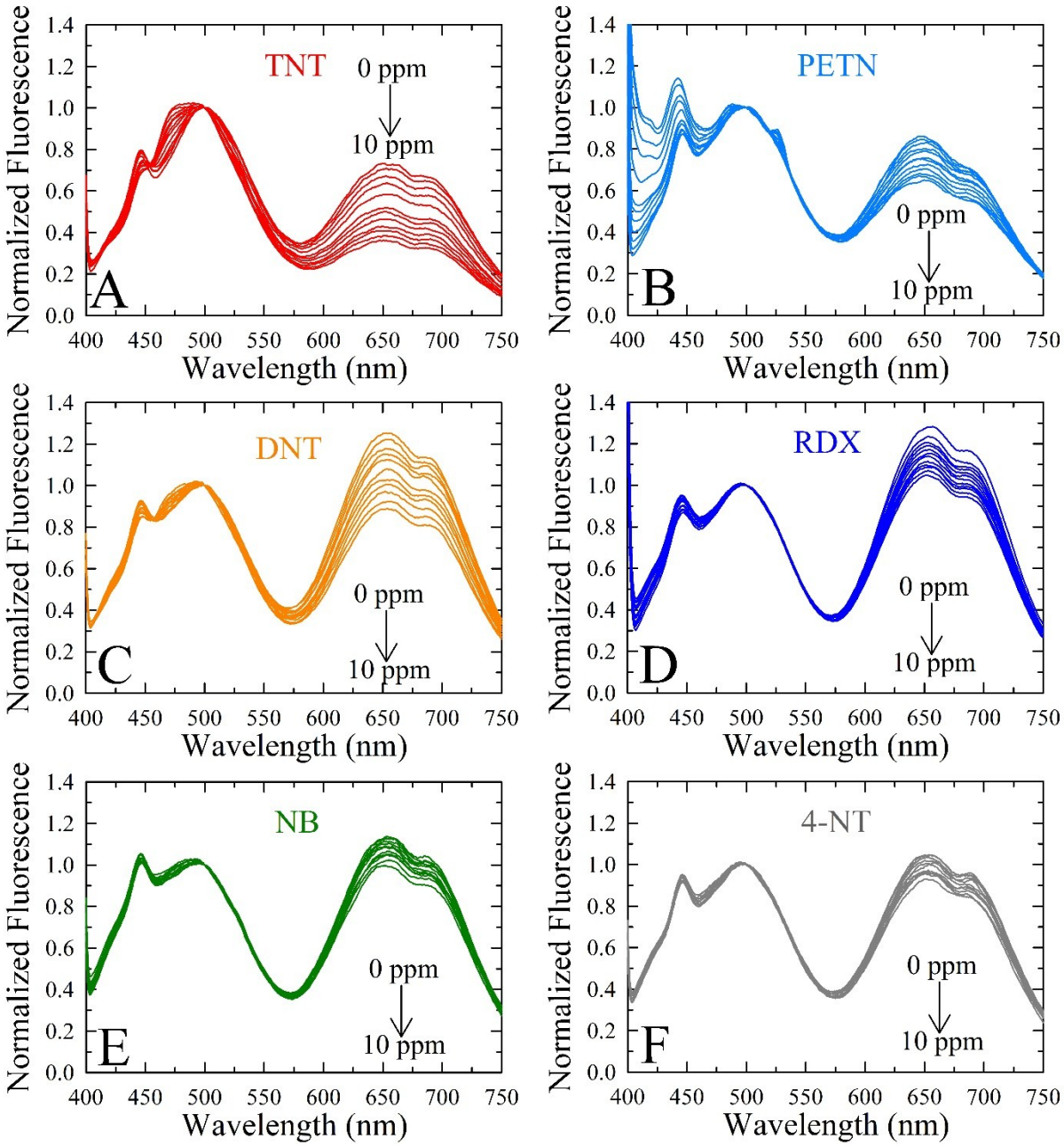

Fig. S6 Representative normalized fluorescence emission spectra (λ_{ex} = 390 nm) of the dual-MNC sample in the presence of increasing quantities (0–10 ppm) of (A) TNT, (B) PETN, (C) DNT, (D) RDX, (E) NB, and (F) 4-NT. All spectra were normalized to the CuNCs@GSH emission peak (i.e., 500 nm).

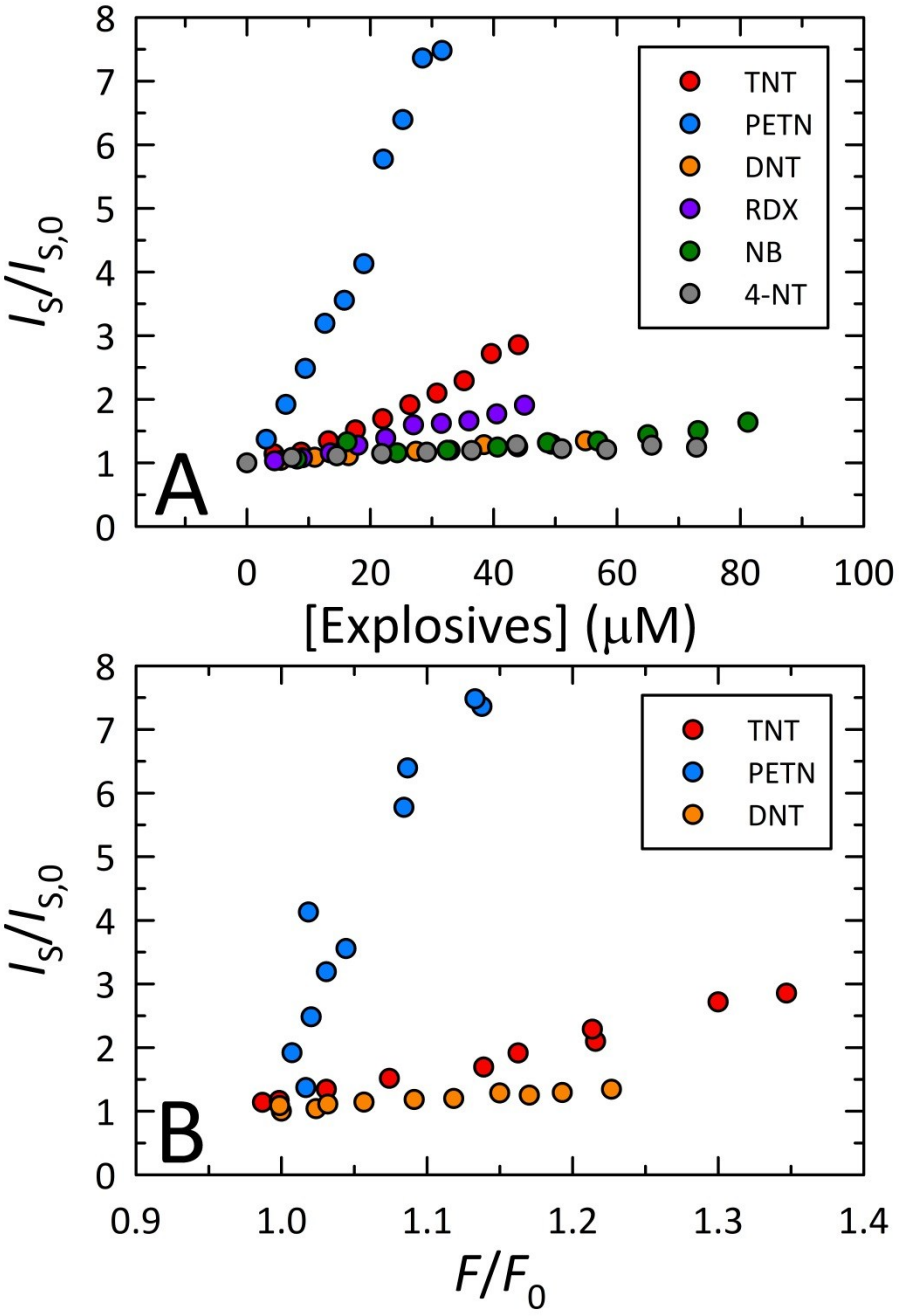

Fig. S7 (A) Integrated intensity of the double-Rayleigh scattering peak in the presence of quencher (I_S) ratioed to the integrated intensity of the double-Rayleigh scattering peak in the absence of quencher ($I_{S,0}$) and plotted against the concentration of explosive present (λ_{ex} = 390 nm; scattering peak integrated from 750–800 nm). The results show increased scattering, especially in the presence of TNT, PETN, and DNT, which eludes to the possible aggregation of Cu(I)-GSSG complexes or deposition of CuNCs@GSH onto BSA, leading to an enhancement of the CuNCs@GSH emission through an AIEE mechanism. (B) The ratioed integrated intensities of the double-Rayleigh scattering peaks plotted against the integrated emission enhancement (F/F_0) of the CuNCs@GSH, further highlighting the proposed AIEE phenomenon. All spectra used to generate panels A and B were integrated over 50-nm slices centered about their respective emission or scattering maxima.

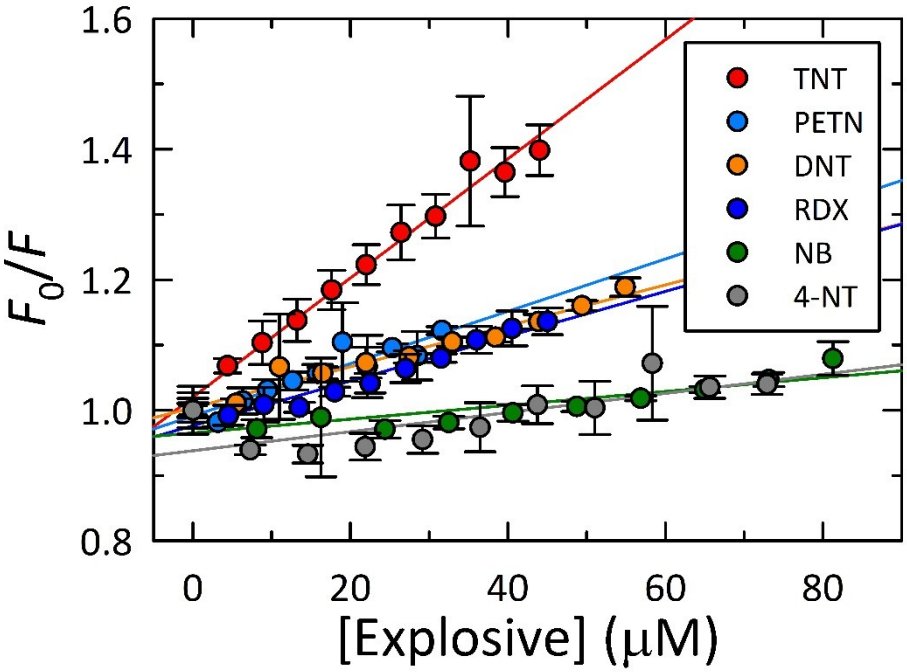

Fig. S8 Stern-Volmer fits of the fluorescence quenching of AuNCs@BSA by explosives. In this plot, F_0/F is the ratio of the integrated AuNCs@BSA fluorescence in the absence (F_0) and presence (F) of quencher. The fluorescence emission was integrated over 50 nm slices centered at 650 nm.

References

1. X. Chen and G. A. Baker, *Analyst*, 2013, **138**, 7299-7302.
2. X. Chen, J. B. Essner and G. A. Baker, *Nanoscale*, 2014, **6**, 9594-9598.